Geochimica et Cosmochimica Acta, Vol. 68, No. 24, pp. 5013–5025, 2004

0016-7037/04 $30.00 + .00

doi:10.1016/j.gca.2004.06.036

Effect of boron on the water speciation in (alumino)silicate melts and glasses

BURKHARD C. SCHMIDT*†
Bayerisches Geoinstitut, Universität Bayreuth, D-95440 Bayreuth, Germany

(*Received January* 14, 2004; *accepted in revised form June* 21, 2004)

Abstract—The investigation of hydrous boro(alumino)silicate melts and glasses with near infrared (NIR) spectroscopy revealed an important effect of boron on the water speciation. In the NIR spectra of B-bearing glasses new hydroxyl-related bands develop at the high frequency side of the 4500 cm^{-1} peak. In $NaAlSi_3O_8 + B_2O_3$ glasses this new peak is present as a shoulder at 4650 cm^{-1}, and in $NaAlSi_3O_8$-$NaBSi_3O_8$ (Ab-Rd) glasses it appears as a resolved peak at 4710 cm^{-1}. These bands increase with increasing boron concentration, suggesting that they are due to B-OH complexes. Furthermore, the variations in the NIR spectra indicate that with increasing B-content, but constant total water concentration, the amount of structurally bonded hydroxyl groups increases at the expense of molecular H_2O. For example, at a total water concentration of 4 wt.%, pure Rd-glass contains ~50% more water as hydroxyl groups than pure Ab-glass.

In-situ NIR spectroscopy at high *P* and *T* using a hydrothermal diamond-anvil cell was used to gain information about the temperature dependence of the water speciation in $NaBSi_3O_8$ melts. The data demonstrate the conversion of molecular H_2O to hydroxyl groups with increasing temperature. However, a fully quantitative evaluation of the high *T* spectra was hampered by problems with defining the correct baseline in the spectra. As an alternative approach annealing experiments on a Rd-glass containing 2.8 wt.% water were performed. The results confirm the conversion of H_2O to OH groups with increasing *T,* but also suggest that the OH groups represented by the 4710 cm^{-1} peak (B-OH) participate much less in the conversion reaction compared to X-OH, represented by the 4500 cm^{-1} peak. *Copyright © 2004 Elsevier Ltd*

1. INTRODUCTION

Boron is only a minor component in natural magmas, but can be significantly enriched during the late magmatic or pegmatitic stage of granitic intrusions, where the B_2O_3-concentration can reach several wt.% (e.g. London, 1997; Thomas et al., 2003). In such melts boron lowers considerably the melting temperature and viscosity (Chorlton and Martin, 1978; Pichavant, 1981, 1987; Dingwell et al., 1992) and leads to a significant increase of the water solubility (Pichavant, 1987; Holtz et al., 1993; Romano et al., 1995a). Although there is a great number of structural investigations of anhydrous borosilicate glasses for technical applications (see Dingwell et al., 1996, for review), little is known about the structural interaction between water and boron bearing melts and glasses. In B-free silicate melts and glasses water dissolves in the form of at least two different species, H_2O molecules (H_2Omol) and structurally bonded OH groups (e.g. Scholze, 1960; Bartholomew and Schreuers, 1980; Stolper, 1982; Eckert et al., 1988). Using near infrared (NIR) spectroscopy the concentrations of these two species can be determined from the well-resolved absorption bands at ~5200 cm^{-1} (H_2Omol) and 4500 cm^{-1} (X-OH). For hydrous B-bearing silicate glasses there existed only the NIR spectroscopic study of Romano et al. (1995a), who investigated hydrous haplogranite (HPG8) glasses to which up to 19 wt.% B_2O_3 were added. These authors reported the appearance of a new absorption band at 4650 cm^{-1}, which was stabilised with increasing B-content, suggesting that this band is due to boron-hydroxyl complexes. The data further demonstrated that the water speciation in these B-bearing glasses was shifted towards higher hydroxyl contents on the expense of molecular water. Apart of the study of Romano et al. (1995a) no other information about the structure of hydrous boro(alumino)silicate melts and glasses (from NMR or Raman spectroscopy) or the water speciation in other borosilicate compositions is available in the literature.

It is known that the water speciation in silicate glasses does not correspond to that in the melt phase at high temperatures, but rather to that at the fictive temperature (T_f). Above that temperature melt relaxation is too fast to preserve equilibrium speciation during quench (Dingwell and Webb, 1990). For various aluminosilicate melt compositions the equilibrium $H_2O_{melt} + O_{melt} = 2\ OH_{melt}$ was shown to shift significantly to the right above the glass transition with increasing temperature (e.g. Nowak and Behrens, 1995; Shen and Keppler, 1995; Zhang et al., 1995, 1997; Ihinger et al., 1999; Sowerby and Keppler, 1999; Nowak and Behrens, 2001). In order to relate physical properties of a silicate melt to its structure, it is therefore necessary to understand the temperature dependence of the water speciation. The temperature dependence of the water speciation was studied with various experimental approaches using NIR spectroscopy: (1) in-situ NIR measurements on silicate melts at high *T* (and *P*) (e.g. Nowak and Behrens, 1995; Shen and Keppler, 1995; Sowerby and Keppler, 1999); (2) annealing of hydrous glasses nearby the glass transition followed by rapid quench (e.g. Stolper, 1989; Zhang et al., 1995, 1997; Ihinger et al., 1999); (3) variation of the cooling rate from superliquidus conditions (e.g. Romano et al., 1995b; Zhang et al., 2000; Behrens and Nowak, 2003); (4) determining T_f for a series of hydrous glasses along the join albite-orthoclase from fluid inclusions and relating it to the water speciation (Romano et al., 1995b). The last three methods

* Author to whom correspondence should be addressed (burkhard.schmidt@geo.uni-goettingen.de).
† *Present address:* Experimentelle und Angewandte Mineralogie Universität Göttingen, Goldschmidtstr. 1 D-37077 Göttingen, Germany

Table 1. Experimental conditions and results.

Composition	Sample	Pressure (bar)	Temperature (°C)	Duration (h)	Results	Density[a] (g/L)	c_{water} NMR[b] (wt.%)
Rd100	Rd100-0.5H2	2000	1100	94	cg, bf	2483	nd
	Rd100-1H2	2000	1100	94	cg, bf	2467	nd
	Rd100-2H	2000	1000	96	cg, bf	2445	2.25
	Rd100-2.5H	2000	1100	96	cg, bf	nd	2.80
	Rd100-4H	2000	1000	120	cg, bf	2420	4.22
	Rd100-5H	2000	1000	94	cg, bf	2400	5.26
	Rd100-6H	2000	1000	91	cg, bf	2379	6.51
	Rd100-7H	2000	1000	94	cg, bf	2359	7.64
	Rd100-8H	2000	1000	91	cg, bf	2342	8.60
Ab25Rd75	Rd75-4H	2000	1000	118	cg, bf	2405	4.35
Ab50Rd50	Rd50-4H	2000	1000	96	cg, bf	2372	4.22
Ab75Rd25	Rd25-0.5H	2000	1100	96	cg, bf	nd	nd
	Rd25-1H	2000	1100	96	cg, bf	2392	1.11
	Rd25-2H	2000	1100	95	cg, bf	2387	2.09
	Rd25-3H	2000	1100	96	cg, bf	2385	2.99
	Rd25-4H	2000	1000	120	cg, bf	2356	4.28
	Rd25-6H	2500	1000	95	cg, bf	2325	6.17
	Rd25-8H	2500	1000	95	cg, bf	2301	8.00
Ab100	Ab-1H	2000	1100	100	cg, fb	nd	nd
	Ab-2H	2000	1100	100	cg, fb	nd	nd
	Ab-3H	2000	1000	95	cg, fb	nd	nd
	Ab-4H	2000	1000	99	cg, bf	2342	4.40
	Ab-5H	2250	1000	97	cg, fi, ih	nd	nd
	Ab-6H	2250	1000	97	cg, fi, ih	nd	nd
Ab-5B	Ab-5B-4H	2000	1000	96	cg, bf	2321	4.27
Ab-9B	Ab-9B-4H	2000	1000	96	cg, bf	2301	4.40
Ab-17B	Ab-17B-1H2	2000	1000	95	cg, bf	2313	1.29
	Ab-17B-2H2	2000	1000	95	cg, bf	2286	2.39
	Ab-17B-3H	2000	1000	95	cg, bf	nd	3.52
	Ab-17B-4H	2000	1000	136	cg, bf	2271	4.49
	Ab-17B-7H	2000	850	91	cg, bf	nd	6.92

nd: not determined; cg: clear glass; bf: bubble free; fb: few air bubbles; fi: fluid inclusions; ih: inhomogeneous water distribution (based on NIR spectroscopy).

[a] Measured glass densities, uncertainty is 1%.

[b] c_{water} determined with static ^{1}H NMR spectroscopy, uncertainty is 3%.

provide samples with a range of T_f at which the distribution of hydrous species is frozen in, thus IR spectra are obtained from glasses at ambient temperature. Only in-situ measurements (method (1)) can yield water speciation data for temperatures far above the glass transition in a silicate liquid. However, consistent data on the effect of temperature on the water speciation can be obtained by the different approaches (1 to 4), as it was recently demonstrated by Behrens and Nowak (2003).

The study presented here is part of a larger investigation on the effects of boron on the structure of hydrous aluminosilicate melts and glasses and focuses on the determination of the influence of boron on the water speciation with NIR spectroscopy. The temperature dependence of the water speciation in the melt phase was studied with in-situ NIR measurements and annealing experiments. The description of the network structure of the investigated melts and glasses from NMR and Raman spectroscopy is presented elsewhere (Schmidt et al., 2004).

2. EXPERIMENTAL METHODS

2.1. Sample Preparation

Two systems with albitic base composition were investigated. System I consists of albite glass ($NaAlSi_3O_8$) to which different amounts of B_2O_3 were added (Ab-xB series). System II consists of glasses along the join $NaAlSi_3O_8$-$NaBSi_3O_8$ (albite-reedmergnerite), i.e. the aluminium was progressively substituted by boron (Ab-Rd series).

For the Ab-xB series four glass compositions containing 0 to 15.6 wt.% B_2O_3 were prepared: Ab100, pure albite, $NaAlSi_3O_8$; Ab-5B, 4.8 wt.% B_2O_3, $NaAlB_{0.38}Si_3O_{8.57}$; Ab-9B, 8.9 wt.% B_2O_3, $NaAlB_{0.74}Si_3O_{9.11}$ and Ab-17B, 15.6 wt.% B_2O_3, $NaAlB_{1.39}Si_3O_{10.09}$. Boron concentrations were determined by electron microprobe analysis (Schmidt et al., 2004). The Ab-Rd glass series consists of five compositions: Ab100, pure albite; Ab75Rd25, $NaAl_{0.75}B_{0.25}Si_3O_8$; Ab50Rd50, $NaAl_{0.5}B_{0.5}Si_3O_8$; Ab25Rd75 $NaAl_{0.25}B_{0.75}Si_3O_8$ and Rd100, pure reedmergnerite $NaBSi_3O_8$. Dry glasses were prepared in a Pt crucible for 10 to 60 min at 1200 to 1600°C and 1 atm from mixtures of powdered SiO_2, Al_2O_3, Na_2CO_3 and H_3BO_3. After quenching the melts to glasses by dipping the bottom of the crucible in water, the glasses were re-ground in an automatic mortar and re-melted at the same conditions for further homogenisation. Hydrous glasses containing 0.5 to 8.6 wt.% water were prepared from the dry starting glasses and distilled water in hydrothermal experiments at 2 to 2.5 kbar, 850 to 1100°C for 91 to 136 h (Table 1). The desired proportions of glass and water were sealed into Pt-capsules by welding. To minimise water loss during welding, the capsules were wrapped in wet tissue paper and cooled in liquid nitrogen. After welding, the capsules were placed in a drying oven at 150°C for at least 24 h to homogeneously distribute the water and to check for weight loss. The hydration experiments were performed in vertically operating, rapid quench TZM (titanium-zirconium-molybdenum alloy) cold-seal pressure vessels with Ar as pressure medium. The sample capsules were placed in the hot top part of the vessels and were kept in position by a filler rod, which was held by an external magnet. Sample temperatures were determined by calibration of the temperature difference between the furnace temperature and

Table 2. Sample characterisation and results of NIR spectroscopy.

Sample	c_{water} (wt.%)	Density[a] (g/L)	A (5230)[b] (mm^{-1})	A (4710)[b] (mm^{-1})	A (4500)[b] (mm^{-1})	c_{H_2O} (5230) (wt.%)	c_{OH1} (4710) (wt.%)	c_{OH2} (4500) (wt.%)	c_{water} IR (wt.%)
Rd100-0.5H2	nd	2478	0.0012 (02)	0.0292 (5)	0.0568 (10)	0.01	0.16	0.31	0.48
Rd100-1H2	nd	2468	0.0160 (11)	0.0636 (35)	0.1160 (35)	0.09	0.35	0.65	1.09
Rd100-2H	2.25 (7)[c]	2449	0.0632 (14)	0.1154 (45)	0.2088 (53)	0.34	0.65	1.17	2.16
Rd100-2.5H	2.80 (8)[c]	2440	0.1084 (23)	0.1464 (83)	0.2496 (99)	0.58	0.82	1.41	2.81
Rd100-4H	4.22 (13)[c]	2417	0.2532 (15)	0.2047 (22)	0.3226 (27)	1.38	1.16	1.83	4.37
Rd100-5H	5.26 (16)[c]	2400	0.3771 (25)	0.2353 (49)	0.3487 (60)	2.07	1.35	2.00	5.41
Rd100-6H	6.51 (20)[c]	2380	0.5119 (25)	0.2667 (37)	0.3693 (50)	2.83	1.54	2.13	6.50
Rd100-7H	7.64 (23)[c]	2361	0.6453 (17)	0.2925 (23)	0.3898 (44)	3.59	1.70	2.27	7.56
Rd100-8H	8.60 (26)[c]	2346	0.7657 (46)	0.3138 (13)	0.3994 (26)	4.29	1.84	2.34	8.47
Rd25-0.5H	nd	2407	0.0057 (02)	0.0121 (02)	0.0742 (02)	0.03	0.07	0.42	0.52
Rd25-1H	1.11 (3)[c]	2398	0.0286 (02)	0.0287 (05)	0.1378 (12)	0.13	0.16	0.78	1.07
Rd25-2H	2.09 (6)[c]	2385	0.1253 (07)	0.0497 (17)	0.2227 (19)	0.57	0.28	1.26	2.11
Rd25-3H	2.99 (9)[c]	2372	0.3000 (01)	0.0688 (27)	0.2505 (31)	1.38	0.39	1.43	3.20
Rd25-4H	4.28 (13)[c]	2354	0.4115 (16)	0.0836 (54)	0.3076 (55)	1.91	0.48	1.77	4.16
Rd25-6H	6.17 (19)[c]	2328	0.7470 (13)	0.1101 (07)	0.3409 (15)	3.51	0.64	1.98	6.13
Rd25-8H	8.00 (24)[c]	2302	1.0572 (33)	0.1308 (11)	0.3594 (10)	5.02	0.77	2.11	7.90
Ab-1H-B[e]	1.16 (6)[d]	2368	0.0566 (04)		0.1429 (11)	0.25		0.88	1.13
Ab-1H-T[e]	1.14 (6)[d]	2368	0.0550 (08)		0.1413 (14)	0.25		0.87	1.12
Ab-2H-B[e]	2.17 (11)[d]	2354	0.1797 (10)		0.2090 (15)	0.25		1.30	2.10
Ab-2H-T[e]	2.25 (11)[d]	2353	0.1958 (04)		0.2152 (09)	0.25		1.34	2.21
Ab-3H-B[e]	3.21 (16)[d]	2340	0.3488 (13)		0.2541 (36)	0.25		1.59	3.15
Ab-3H-T[e]	3.33 (17)[d]	2338	0.3620 (32)		0.2533 (23)	0.25		1.59	3.21
Ab-4H	4.13 (21)[d]	2327	0.4629 (12)		0.3165 (46)	0.25		1.99	4.08
Ab-5H-B[e]	5.32 (27)[d]	2311	0.6608 (64)		0.3369 (85)	0.25		2.14	5.13
Ab-5H-T[e]	6.66 (33)[d]	2292	0.9070 (92)		0.3583 (103)	0.25		2.29	6.44
Ab-6H-B[e]	5.51 (28)[d]	2308	0.7036 (55)		0.3358 (86)	0.25		2.13	5.33
Ab-6H-T[e]	5.75 (29)[d]	2305	0.7424 (46)		0.3554 (59)	0.25		2.26	5.63

nd: not determined. Maximum uncertainty of c_{water} determination by NMR and NIR and 1σ for the absorbances of multiple NIR spectra are given in parenthesis. Uncertainty based on reproducibility is 0.0003 cm for thickness and 1% for the density.

[a] Glass density calculated from linear regression of multiple, experimental density measurements: Rd-xH glasses: $\rho = 2486 - 16.3 \cdot c_{water}$, Rd25-xH glasses: $\rho = 2414 - 14.0 \cdot c_{water}$, Ab-xH glasses: $\rho = 2384 - 13.8 \cdot c_{water}$ (Behrens et al., 1996).

[b] Peak heights normalised to 1 mm sample thickness.

[c] Water contents determined by static ^{1}H NMR spectroscopy, the maximum error is estimated to be 3%.

[d] Water contents determined by NIR spectroscopy, following the evaluation method of Behrens et al. (1996), the maximum error is estimated to be 5% (see text for details).

[e] -B and -T at the end of sample names correspond to bottom and top part of the sample cylinder from which the doubly polished sections were prepared.

an internal thermocouple at pressure. The maximum error on temperature is ±20°C. Pressures were measured with pressure gauges and are accurate to within ±50 bars. Quenching was close to isobaric and occurred within a few seconds by dropping the sample capsule from the hot top of the vessel into the water cooled part of the pressure seal by removing the magnet, which held the filler rod and the sample (estimated quench rates were 100–200°C/s). All capsules were weighed before and after experiments to ensure that no leaks occurred during the runs. Total water contents of most of the quenched glasses were determined with static ^{1}H NMR spectroscopy following the procedures described in Schmidt et al. (2001).

2.2. NIR Micro-Spectroscopy

Infrared absorption spectra were obtained in the spectral range 2000 to 8000 cm^{-1} using a Fourier transform (FT) - IR spectrometer (Bruker™IFS120HR) and an infrared microscope (type A590) with reflecting optics, a cassegrainian objective (15×) and a MCT (HgCdTe) detector. Spectra were recorded using a tungsten white light source and a CaF_2 beamsplitter for the NIR spectral region. Spectra were measured on doubly polished glass plates of 0.5 to 1.0 mm thickness, which were positioned on a pinhole. The analysed spot was 100 μm in diameter. Typically spectra were acquired in 200 scans with 4 cm^{-1} spectral resolution. The thickness of the doubly polished glass sections was measured with a precision of 3 μm using digital micrometer (Mitutoyo). Glass densities, necessary for the quantitative evaluation of the NIR spectra, were determined with the buoyancy method, i.e. measuring the sample weights in air and in a fluid with known density (ethanol) on a Mettler Toledo AG204 balance (Mettler Toledo density determination kit). The error of the density determinations is <1%.

2.3. In-Situ NIR Micro Spectroscopy

NIR spectra of hydrous Rd100 melt at high pressures and temperatures were obtained using a hydrothermal diamond anvil cell (HDAC; Basset et al., 1993), as modified by Shen and Keppler (1995). A more detailed description of the HDAC setup can be found in Sowerby and Keppler (1999). For the experiment a chip of hydrous glass (e.g. 5 wt.% water) was placed into the sample chamber of the Re gasket (bore hole with initial diameter of 500 μm, thickness 250 μm), together with water and an air bubble. To avoid problems arising from dissolution of melt components in the water pressure medium at high P and T, the fraction of loaded glass was as high as possible. Upon heating the cell, the fluid phase homogenised and at higher temperatures (500–700°C) the glass melted and the gasket deformed. Then the experiment was quenched by switching off the power of the furnaces. The heating and cooling procedure was repeated until the melt contacts the upper and lower anvils and the gaskets did not further deform. In such experiments the melt occupied >70% of the sample chamber volume and was in contact with the gasket. The loaded HDAC was then transferred to the microscope of the IR spectrometer and heated to 800°C. NIR

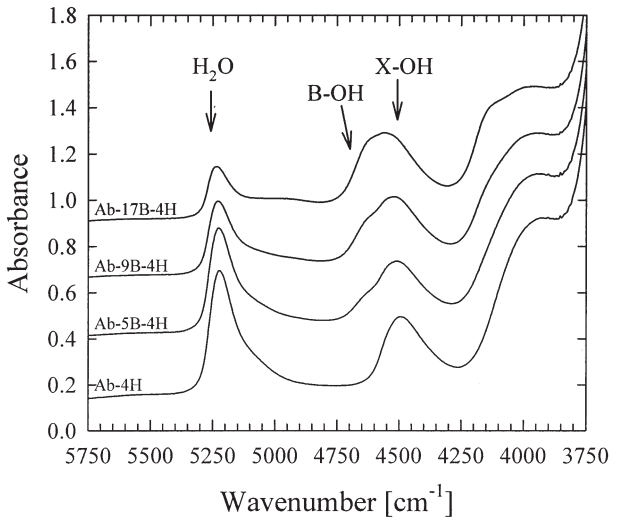

Fig. 1. NIR spectra of $NaAlSi_3O_8$ + B_2O_3 glasses containing 4.4 ± 0.1 wt.% water (series Ab-xB- 4H). The spectra are normalised to a sample thickness of 1 mm and are shifted in intensity for clarity.

spectra were taken every 100 to 200°C during heating and every 50°C to ~330°C during cooling. The analysed spot had a diameter of 60 μm and was located close to the melt-gasket contact, furthest away from the melt-fluid interface to avoid problems of melt dehydrating upon cooling, as the pressure decreases with decreasing temperature (the *P, T* path in a HDAC follows a water isochore; Basset et al., 1993).

2.4. Annealing Experiments

Annealing experiments were performed on hydrous Rd100 glass containing 2.8 wt.% water (Rd100-2.5H). The glass cylinder obtained from the hydration experiment was cut into slices, which were polished on both sides to a thickness of ~1 mm. These glass wafers were placed in a pre-heated alumina crucible into box furnace next to a chromel-alumel thermocouple. Depending on temperature, which ranged from 300 to 555°C, the samples were held for 2 to 5040 min in the furnace to allow re-equilibration of the hydrous species according to the reaction $H_2O_{melt} + O_{melt} = 2OH_{melt}$. The experiments were terminated by dropping the samples into cold water, resulting in a quenching time of ~1 s. Time series experiments were performed to ensure attainment of equilibrium. The water speciation in the quenched glasses was determined with NIR spectroscopy.

3. RESULTS AND DISCUSSION

3.1. Hydrous $NaAlSi_3O_8$ + B_2O_3 Glasses

The NIR spectra of the hydrous Ab-xB glasses containing 4.4 ± 0.1 wt.% water (series Ab-xB-4H) are shown in Figure 1 in the frequency range between 5750 and 3750 cm^{-1}. The spectra are similar to those of Romano et al. (1995a) for B-containing haplogranitic glasses and indicate significant changes in water speciation with increasing B-content (at constant total water content). The band at 5230 cm^{-1} decreases in intensity reflecting the decrease of dissolved H_2Omol. This observation is consistent with the decreasing Raman intensity of the 1635 cm^{-1} band for this glass series (Schmidt et al., 2004), which is due to bending vibrations of molecular H_2O. On the other hand the X-OH peak at 4500 cm^{-1} develops a shoulder at 4640 cm^{-1} and gains in overall intensity. These features suggest not only an increase of the X-OH concentration at the expense of H_2Omol, but also the presence of an additional X-OH species represented by the NIR absorption 4640 cm^{-1}. Romano et al. (1995a) assigned a similar band in B-bearing haplogranite glasses to B-OH complexes and this assignment is followed here. As AB-xB glasses contain dominantly boron in three-fold coordination (92%–98% B^{III}, determined with ^{II}B magic angle spinning (MAS) NMR spectroscopy; Schmidt et al., 2004), it is likely that the NIR peak at 4640 cm^{-1} is due to B^{III}-OH groups.

Further variations of the NIR spectra upon B-incorporation include the development of additional intensity at the low-frequency tail of the H_2Omol related band at around 4950 cm^{-1} and the appearance of a shoulder at the high-frequency tail of the 4000 cm^{-1} band. The origin of the 4000 cm^{-1} band is still unclear and was previously assigned to combination modes of strongly bonded silanol groups (Wu, 1980), vibrations of H_2Omol (Acocella et al., 1984), or to vibrations involving water molecules and hydroxyl groups (Stolper, 1982). The origin of the high-frequency shoulder at 4150 cm^{-1} for the B-containing glasses cannot be deduced from the present data. Also the origin of the 4950 cm^{-1} band is not clear, but it may be speculated that this band could be due to stronger H-bonded H_2O molecules. However, this is not supported by the Raman spectra in the OH stretching region (Schmidt et al., 2004), which indicate similar distribution of O-H...O hydrogen bonds in all hydrous glasses.

For Ab-17B composition a series of hydrous glasses containing ~1 to 7 wt.% water (series Ab-17B-xH) was prepared to attempt the determination of the IR absorption coefficients and quantitative determination of the water speciation. The NIR spectra of this series are shown in Figure 2. In the spectra of the low water content glasses (Ab-17B-1H2 and Ab-17B-2H2) the presence of the peaks at 4950 and 4150 cm^{-1} is more evident than in those of higher water content glasses. However, as all NIR peaks are overlapping, it is difficult to define a reasonable baseline that could be consistently applied for the entire series. From the spectra of the dry and the low water content glasses it seems that the baseline could be given by a straight line that

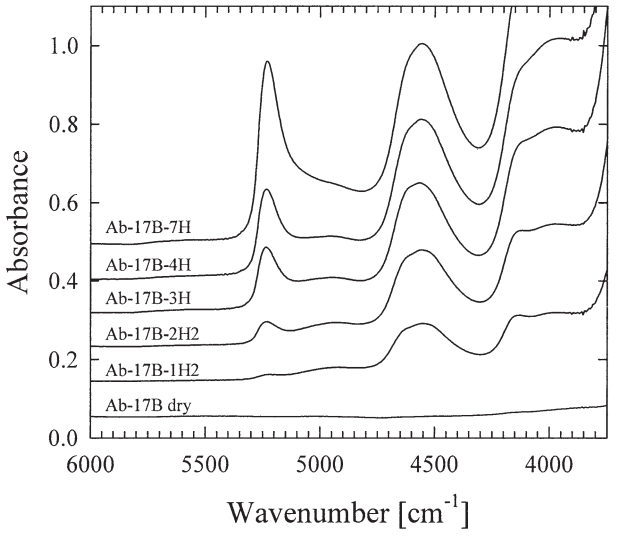

Fig. 2. NIR spectra of Ab-17B glasses containing 1.2 to 7.0 wt.% water (series Ab-17B-xH). The spectra are normalised to a sample thickness of 1 mm and are shifted in intensity for clarity.

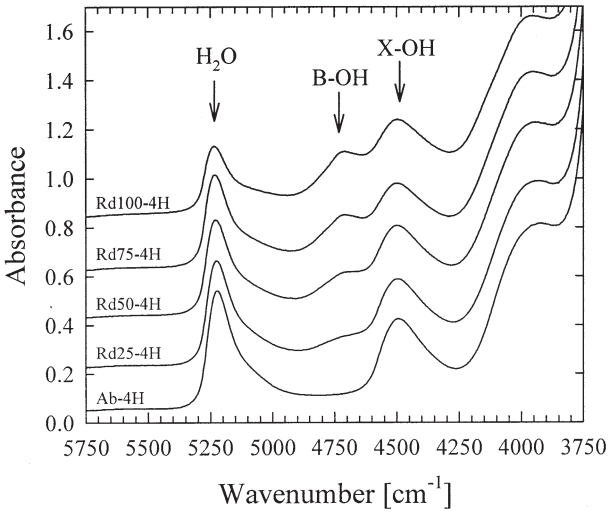

Fig. 3. NIR spectra of $NaAlSi_3O_8$-$NaBSi_3O_8$ glasses containing 4.3 ± 0.1 wt.% water (series AbRd-4H). The spectra are normalised to a sample thickness of 1 mm and are shifted in intensity for clarity.

is defined by the flat intensity between 6000 and 5400 cm^{-1} and extends under the NIR peaks. Applying such baseline to the high water content glasses demonstrates that the additional NIR peaks at 4150, 4640 and 4950 cm^{-1} strongly overlap with the "normal" NIR peaks of X-OH and H_2Omol. Thus, a deconvolution of the spectra would be required to obtain the relative intensities of the individual NIR peaks. In addition to their overlapping character, the NIR peaks do not have well defined peak shapes and always show some degree of asymmetry. Since the outcome of such deconvolutions would probably have a very high error, a further quantitative evaluation and determination of the NIR absorption coefficients was not performed for the Ab-17B-xH series. Nonetheless, the NIR spectra of the hydrous $NaAlSi_3O_8$ + B_2O_3 glasses provided important qualitative conclusions, namely that new OH species are present (probably B-OH) and that the water speciation significantly shifts towards higher hydroxyl concentrations with increasing boron content.

For the Ab-xB-4H glass series (4.4 ± 0.1 wt.% water) Schmidt et al. (2004) presented a quantitative determination of the water speciation (in terms of total OH and H_2Omol) from low temperature, static ^1H NMR spectroscopy. The amount of OH groups was shown to increase from ~1.8 wt.% in Ab-4H to ~3.1 wt.% in Ab-17B-4H, while the amount of H_2Omol decreases correspondingly. These trends compare well with those of Romano et al. (1995a) for hydrous HPG8 glasses containing up to 19 wt.% B_2O_3, for which a more or less linear increase in OH contents from ~1.1 wt.% for the boron free HPG8 glass to ~3.1 wt.% for the HPG8 + 19 wt.% B_2O_3 glass (5 wt.% total water) was reported.

3.2. Hydrous $NaAlSi_3O_8$-$NaBSi_3O_8$ Glasses

The NIR spectroscopic results for Ab-RD glasses are summarized in Table 2. The NIR spectra of the hydrous Ab-Rd glasses containing 4.3 ± 0.1 wt.% water (series AbRd-4H) are shown in Figure 3. In these glasses, the increasing amount of boron leads mainly to the development of a major new peak at 4710 cm^{-1} (compared to 4640 cm^{-1} in Ab-xB), which is resolved from the X-OH peak at 4500 cm^{-1}. A second minor peak may develop at the high frequency tail of the 4000 cm^{-1} band at ~4100 to 4150 cm^{-1}. This peak is most obvious in the spectrum of low water concentration glasses of pure $NaBSi_3O_8$ composition (Fig. 4). As a peak at 4710 cm^{-1} was never reported previously for B-free silicate glasses and the intensity of this peak clearly increases with increasing boron concentration (Fig. 3), it is assigned in analogy to the hydrous Ab-xB glasses to B-OH complexes. The investigation of Ab-Rd glasses with ^{11}B MAS NMR (Schmidt and Dupree, 2002) showed that boron is dominantly four-coordinated (B^{IV}) and that the fraction of B^{IV} strongly increases with increasing water concentration. This may suggest that the NIR peak at 4710 cm^{-1} is due to B^{IV}-OH groups.

Figure 4 shows selected NIR spectra of Rd100 glasses with various water contents (Rd100-xH series). In all spectra the maximum of the 4710 cm^{-1} NIR peak is well resolved from the 4500 cm^{-1} peak, although its base overlaps with the high- and low-frequency tails of the 4500 and 5230 cm^{-1} peaks. The separation of the peak maxima enables at least a semi-quantitative evaluation of the NIR spectra. Water species concentrations can be calculated from NIR spectra using a modified law of Lambert-Beer. It requires the knowledge of the sample thickness and density, as well as the intensities and absorption coefficients of the relevant absorption bands. To obtain the correct peak intensities, the experimental NIR spectra have to be baseline corrected. Usually the baselines applied for NIR spectra of Fe-free, hydrous (alumino)silicate glasses consist of flexicurves (e.g. Stolper, 1982; Newman et al., 1986; Silver and Stolper, 1989; Silver et al., 1990; Romano et al., 1995a; Zhang et al., 1997), straight lines that are defined as tangents to the high- and low-frequency minima of the 5200 cm^{-1} peak and extended below the 4500 cm^{-1} peak (e.g. Behrens et al., 1996; Withers and Behrens, 1999; Nowak and Behrens, 1997; Schmidt et al., 2001) or tangents to the high- and low-fre-

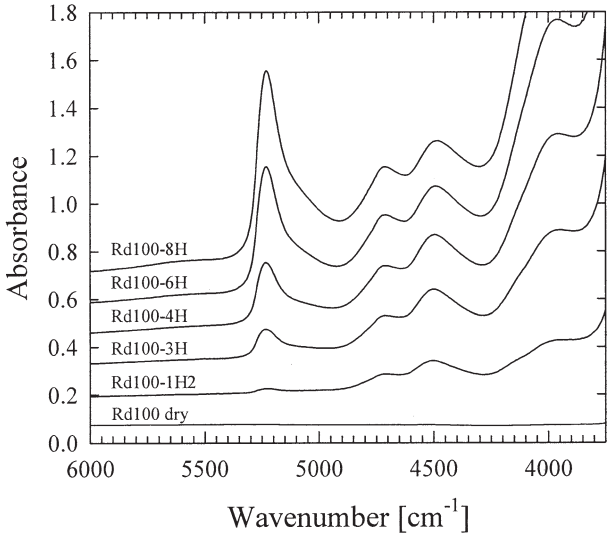

Fig. 4. NIR spectra of $NaBSi_3O_8$ glasses containing 1.1 to 8.6 wt.% water (series Rd100-xH). The spectra are normalised to a sample thickness of 1 mm and are shifted in intensity for clarity.

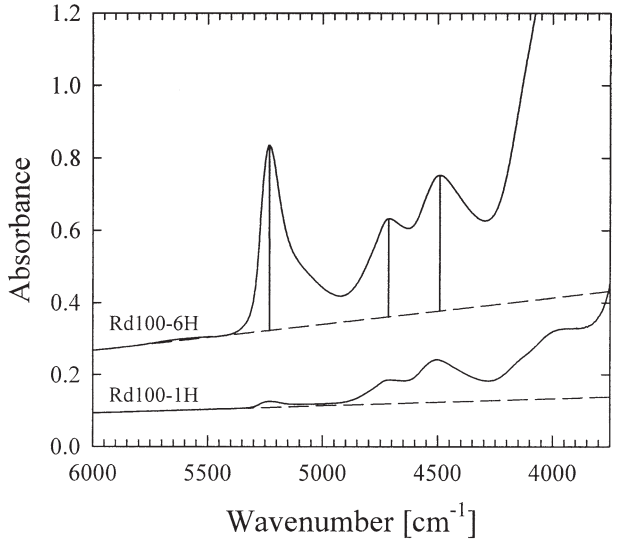

Fig. 5. Spectra evaluation used in this study. The baseline for the NIR spectra was defined by the flat intensity on the high frequency side of the H_2O peak between 5900 and 5400 cm^{-1} and extended underneath the NIR absorption bands. Peak heights were used as intensities.

quency minima of the 5200 and 4500 cm^{-1} peaks (e.g. Withers and Behrens, 1999). The influence of different evaluation methods on the determination of molar absorption coefficients and water speciation were investigated in Withers and Behrens (1999) and Ohlhorst et al. (2001). However, for the NIR spectra presented here, these usually applied baselines could not be used, as they rely on an "intensity-free" region between the H_2O and X-OH peaks, and the spectra of the B-bearing glasses contain an additional peak (B-OH) in this frequency range. For example, flexicurve baselines would have little constraints for their shape underneath the 4710 and 4500 cm^{-1} peaks, thus measured intensities would rely completely on the subjective choice of such baseline. Tangential baselines are not useful as the relative minimum between the H_2O and X-OH peaks (about 4900 cm^{-1} for hydrous Ab-Rd glasses) contains significant intensity from the 5200 cm^{-1} peak (in particular for high water content glasses). Therefore they would yield more or less correct intensities for water-poor (H_2Omol-poor) glasses, but for high water contents the OH peak intensities would be significantly underestimated. The baseline chosen for this study consists of a straight line, that is defined by the "flat absorption" between 5900 and 5430 cm^{-1}, which was extended under the NIR peaks (Fig. 5). This type of baseline is probably not ideal, but could at least consistently be applied to low and high water content glasses. However, one has to be aware that this type of baseline probably overestimates the intensities of the OH peaks (in particular that at 4500 cm^{-1}), due to some overlap with high frequency tails of the 4000 to 4100 cm^{-1} composite peaks and the 3600 cm^{-1} fundamental OH stretching vibration. Although the calibration of the absorption coefficients will compensate this effect to some extent, the extracted OH concentrations will probably be overestimated (see below). For measuring intensities only peak heights were used, as they are less sensitive to the overlapping character of the NIR bands of Ab-Rd glasses than integral intensities. Since NIR peaks have asymmetric shapes with a flatter low-frequency tail, the peak height that is most likely affected by overlap with other bands is that of the 4500 cm^{-1} band, probably resulting in some degree of additional intensity over-estimation.

At first it was attempted to determine the absorption coefficients for all three NIR bands (5230, 4710, 4500 cm^{-1}) independently. This can be done with help of a series of hydrous glasses with known water contents (like Rd100-xH) and a modified law of Lambert Beer that assumes that the total water content is given by the sum of water species represented by the NIR peaks at 5230 (H_2Omol), 4710 (B-OH) and 4500 cm^{-1} (X-OH):

$$\left(\frac{A_{5230}\cdot 18.02}{d\cdot\rho\cdot c_{\text{water}}}\right)=\varepsilon_{5230}-\left(\frac{A_{4710}\cdot 18.02}{d\cdot\rho\cdot c_{\text{water}}}\right)\cdot\frac{\varepsilon_{5230}}{\varepsilon_{4710}}-\left(\frac{A_{4500}\cdot 18.02}{d\cdot\rho\cdot c_{\text{water}}}\right)\cdot\frac{\varepsilon_{5230}}{\varepsilon_{4500}},\quad(1)$$

where A_{5230}, A_{4710} and A_{4500} are the absorbances (peak heights) of the 5230, 4710 and 4500 cm^{-1} NIR peaks, d is the transmitted sample thickness (cm), ρ is the glass density (g/L); c_{water} is the total water concentration (wt.%) and ε_{5230}, ε_{4710} and ε_{4500} are the linear molar absorption coefficients (L/mol · cm) for the relevant bands (referring to mole of dissolved H_2O). Eqn. 1 is an equation for a plane in the three-dimensional space, thus plotting the normalised absorbances (the terms in parentheses) in a 3-D plot and fitting the data to a plane gives the variables ε_{5230}, $\varepsilon_{5230}/\varepsilon_{4710}$ and $\varepsilon_{5230}/\varepsilon_{4500}$ and thus the absorption coefficients. However for the glasses of the Rd100-xH series, the data did not plot on a plane, but only on a straight line in the 3D-space, indicating that the B-OH/X-OH ratios do not vary sufficiently. Even when using data from annealing

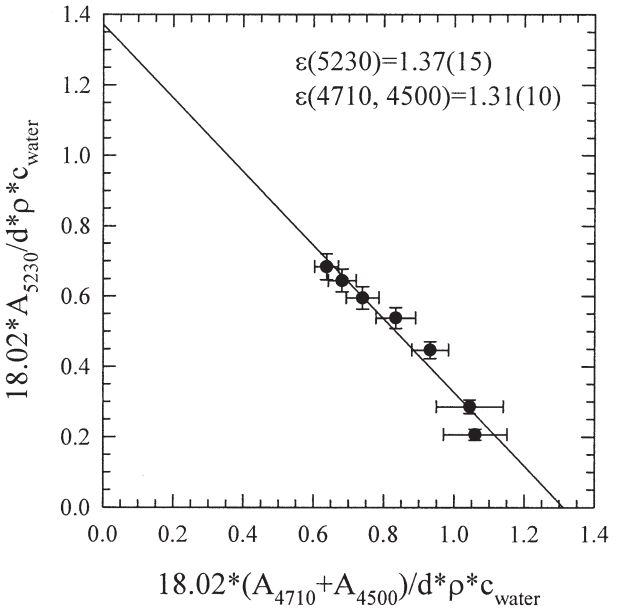

Fig. 6. Calibration plot for the determination of the linear molar absorption coefficients of the NIR absorption bands at 5230, 4710 and 4500 cm^{-1} in Rd100-xH glasses. An equal absorption coefficient was assumed for the OH absorption bands at 4710 and 4500 cm^{-1}. The intercepts of the linear regression with the axes determine the absorption coefficients.

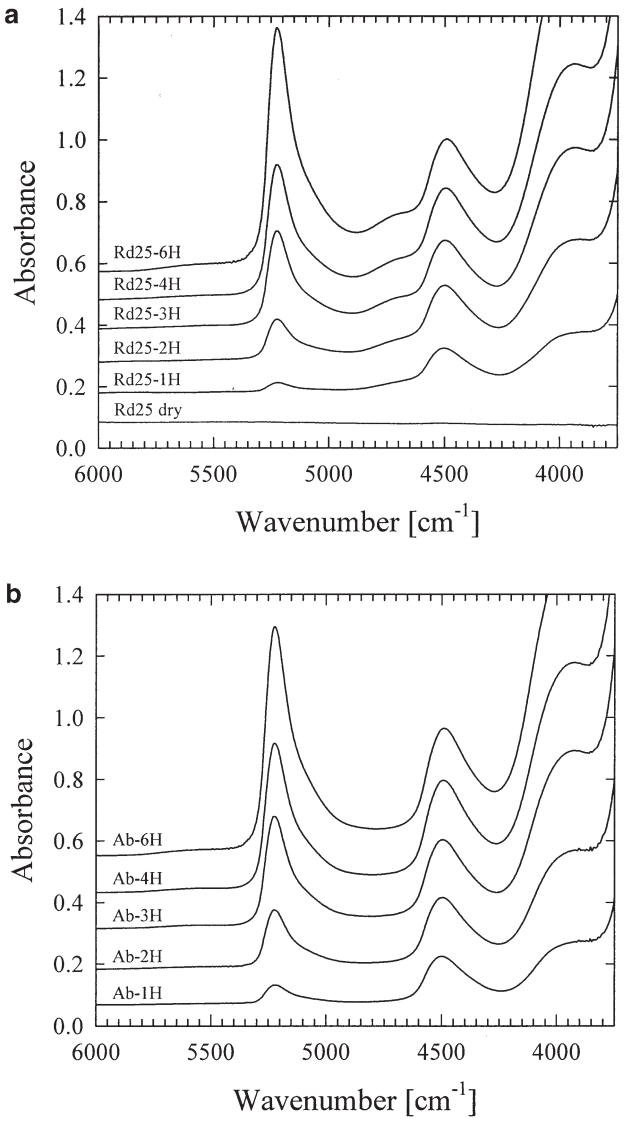

Fig. 7. NIR spectra of Rd25-xH (a) and Ab100-xH (b) glasses. The spectra are normalised to a sample thickness of 1 mm and are shifted in intensity for clarity.

experiments (see below), the B-OH/X-OH variation was not high enough to enable the independent determination of the absorption coefficients with this method.

As a further simplification for the quantitative evaluation of the NIR spectra, a single value for ε_{4710} and ε_{4500} was used, assuming that the absorption coefficients for the combination bands of the various types of structurally bonded hydroxyl groups do not change significantly in such small wavenumber range. Thus, Eqn. 1 simplifies to an equation of a straight line:

$$\left(\frac{A_{5230}\cdot 18.02}{d\cdot\rho\cdot c_{\text{water}}}\right)=\varepsilon_{5230}-\left(\frac{A_{4710+4500}\cdot 18.02}{d\cdot\rho\cdot c_{\text{water}}}\right)\cdot\frac{\varepsilon_{5230}}{\varepsilon_{4710,4500}}. \quad (2)$$

Assuming that all hydrous species present in the glasses are represented by the 5230, 4710 and 4500 cm^{-1} bands, and that the absorption coefficients for these bands are independent on water concentration, the values of ε were obtained from a linear regression of the data in Figure 6. In such graph, the intercepts of the fitted line with the x- and y-axes correspond to the absorption coefficients of the OH and H_2Omol combination bands. The resulting linear molar absorption coefficients for the NIR peaks of Rd100-xH glasses are ε_{5230} = 1.37 and $\varepsilon_{4710,\ 4500}$ = 1.31 L/mol · cm. The maximum error for the linear molar absorption coefficients from the linear regression is 0.15 and 0.1 for ε_{5230} and $\varepsilon_{4710,\ 4500}$, respectively. The assumption of using the same absorption coefficient for the bands at 4710 and 4500 cm^{-1} is probably an over-simplification, as it was demonstrated that the NIR absorption coefficients vary with composition. For example, for glasses with alkali feldspar compositions ($MAlSi_3O_8$, M = Li, Na, K), the linear molar absorption coefficients lie in the ranges 1.13 to 1.58 and 1.12 to 1.87 L/mol · cm for the 4500 and 5200 cm^{-1} peaks, respectively, depending on composition, but also to some smaller extent on the applied baseline (e.g. Silver et al., 1990; Behrens et al., 1996; Withers and Behrens, 1999). Considering the dependency of the absorption coefficients on local structure (bonding), it is therefore likely that also the true absorption coefficients for the 4710 and 4500 cm^{-1} peaks are somewhat different. However it is quite difficult to estimate to what extent ε_{4710} and ε_{4500} may vary. In this sense, the absorption coefficients obtained with Eqn. 2 should be viewed as "effective" or "apparent" absorption coefficients.

Aside of Rd100-xH glasses, two other hydrous glass series were prepared, one with Ab75Rd25 and the other with pure Ab composition (Rd25-xH, 1.1–8.0 wt.% water; Ab100-xH, 1.1–6.4 wt.% water). Selected NIR spectra of these glasses are shown in Figure 7. The Ab100-xH glass series was prepared with the aim to compare the NIR evaluation method applied in this study to conventionally used NIR evaluations. The low water content Ab100-xH glasses contained few small bubbles, probably from residual air trapped in the capsule during synthesis. The samples Ab-5H and Ab-6H contained even bigger bubbles filled with water and CO_2. The reason for CO_2 contamination was probably insufficient drying of the glass powder, which was ground under acetone before synthesis of the hydrous samples. Furthermore, Ab-5H (and Ab-6H to a smaller extent) turned out to be inhomogeneous with respect to water concentration. For Ab100-xH glasses no ^1H NMR data were available to determine total water contents. Water concentrations were determined from the NIR spectra following the evaluation procedures (tangential baseline to the high- and low-frequency minima of the 5200 cm^{-1} peak) and using the linear molar absorption coefficients of Behrens et al. (1996). Due to bubbles in Ab100-xH glasses, the glass densities for this series were not determined experimentally, but were calculated iteratively using a relation between density and water content (Behrens et al., 1996). The evolution of water speciation in Ab100-xH glasses determined using these procedures (not shown) is similar to previously published data on hydrous $NaAlSi_3O_8$ glasses (e.g. Silver and Stolper, 1989; Behrens et al., 1996; Schmidt et al., 2001). The cross-over of OH and H_2O concentrations occurs at ~3 wt.% total water and the levelling-off concentration for OH is ~1.9 wt.% H_2O, a typical number for rapidly quenched glasses (e.g. Silver et al., 1990; Behrens and Nowak, 2003).

The NIR spectra of Rd25-xH, but also those of Ab100-xH glasses, were then evaluated using the same procedures as for

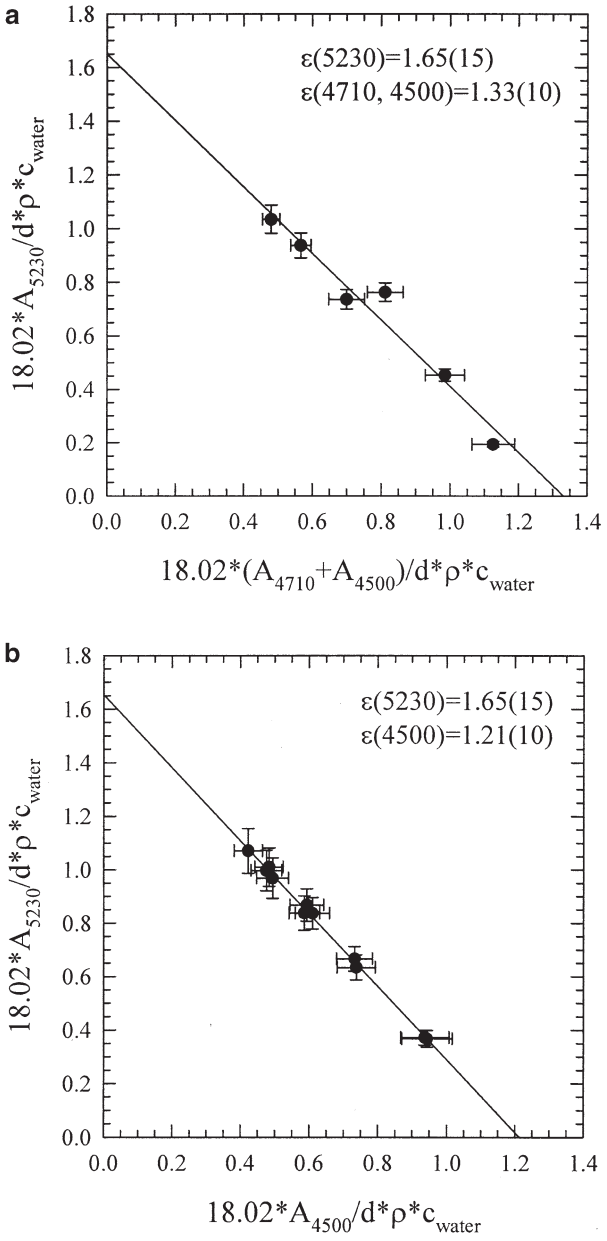

Fig. 8. Calibration plots for the determination of the linear molar absorption coefficients of the NIR absorption bands of Rd25-xH (a) and Ab100-xH (b) glasses. An equal absorption coefficient was assumed for the OH absorption bands at 4710 and 4500 cm^{-1} of Rd25-xH. The intercepts of the linear regression with the axes determine the absorption coefficients.

Rd100-xH glasses, and the plot of normalised absorbances is given in Figure 8. The resulting linear molar absorption coefficients for the NIR peaks of Rd25-xH glasses are ε_{5230} = 1.65 (15) and $\varepsilon_{4710,\ 4500}$ = 1.33 (10) L/mol · cm, and for Ab-xH glasses they were determined to be ε_{5230} = 1.65 (15) and ε_{4500} = 1.21 (10) L/mol · cm. The numbers in parentheses are the estimated maximum errors from the linear regressions. Comparing the latter data to the absorption coefficients for hydrous Ab glasses determined using conventional baseline constructions (ε_{5230} = 1.46–1.49 and ε_{4500} = 1.20–1.34 L/mol · cm; Behrens et al., 1996; Withers and Behrens, 1999) shows that ε_{5230} from this study is significantly higher, while ε_{4500} is similar to previous studies. As a consequence the calculated H_2O concentrations will be smaller and those for OH groups will be enhanced. This is demonstrated in Figure 9a where the OH concentration levels off at ~2.3 wt.% compared to 1.9 wt.% using a conventional baseline and corresponding absorption coefficients for the spectra evaluation. Therefore, the error of the applied NIR evaluation method may be as high as 20% for the OH concentrations.

The calculated water speciations in Rd25-xH and Rd100-xH glasses are presented in Figures 9b and 9c. It is obvious that boron considerably affects the water speciation, i.e. with increasing boron concentration the amount of structurally bonded OH groups increases significantly, even taking into account a large relative error resulting from the NIR evaluation. For example, of 4 wt.% total water 2.0 wt.% are dissolved as OH groups in Ab100 glass, whereas 2.2 and 2.9 wt.% are dissolved as OH groups in Ab75Rd25 (~3 wt.% B_2O_3) and Rd100 (~15 wt.% B_2O_3) glass, respectively. These values compare relatively well with water speciation data for Ab-xB glasses containing 4.4 wt.% total water, obtained from low temperature, static ^1H NMR spectroscopy (Schmidt et al., 2004). For example, the OH concentrations in Ab-5B-4H (~5 wt.% B_2O_3) and Ab-17B-4H (~16 wt.% B_2O_3) are increased by 0.2 wt.% and 1.3 wt.%, respectively, relative to pure Ab glass. Although the structures of Ab-xB and Ab-Rd glasses are somewhat different (dominantly trigonal BO_3 units, not expelling Al from tetrahedral sites in Ab-xB) (Schmidt et al., 2004) and dominantly tetrahedral BO_4 in replacing AlO_4 tetrahedra in Ab-Rd glasses, it seems that boron has a similar effect on the water speciation in both systems. This is also in accord with the data of Romano et al. (1995a) for HPG8 + B_2O_3 glasses, who reported a similar increase of OH concentrations with increasing B-content. Thus, the good agreement between these data sets may give support to the quantification of total OH and H_2Omol presented here. However, one has to be aware that the total OH concentration may be better constraint by the applied calibration than the relative concentrations of B-OH and X-OH that are shown in Figure 9.

In contrast to Ab glasses, the hydroxyl concentration threshold is not even reached for the Ab75Rd25 and Rd100 glasses with the highest water contents (8 and 8.5 wt.%, respectively). It is also interesting that most of the additional OH concentrations are provided by B-OH, while the evolution of the X-OH contents with increasing total water content seem to be relatively similar for all glass compositions, provided that the systematic evaluation errors are similar for all glass compositions. Even if the errors for the determination of the absolute species concentrations are higher than for previously studied B-free glasses (due to higher uncertainties with the applied baseline correction and the assumption of a single value for the absorption coefficients of the 4710 and 4500 cm^{-1} peak), the data clearly demonstrate that the water speciation in B-bearing glasses is significantly shifted towards higher hydroxyl concentrations.

3.3. In-Situ NIR Spectroscopy

The temperature dependence of the water speciation in hydrous Rd100 melt was investigated with help of experiments in

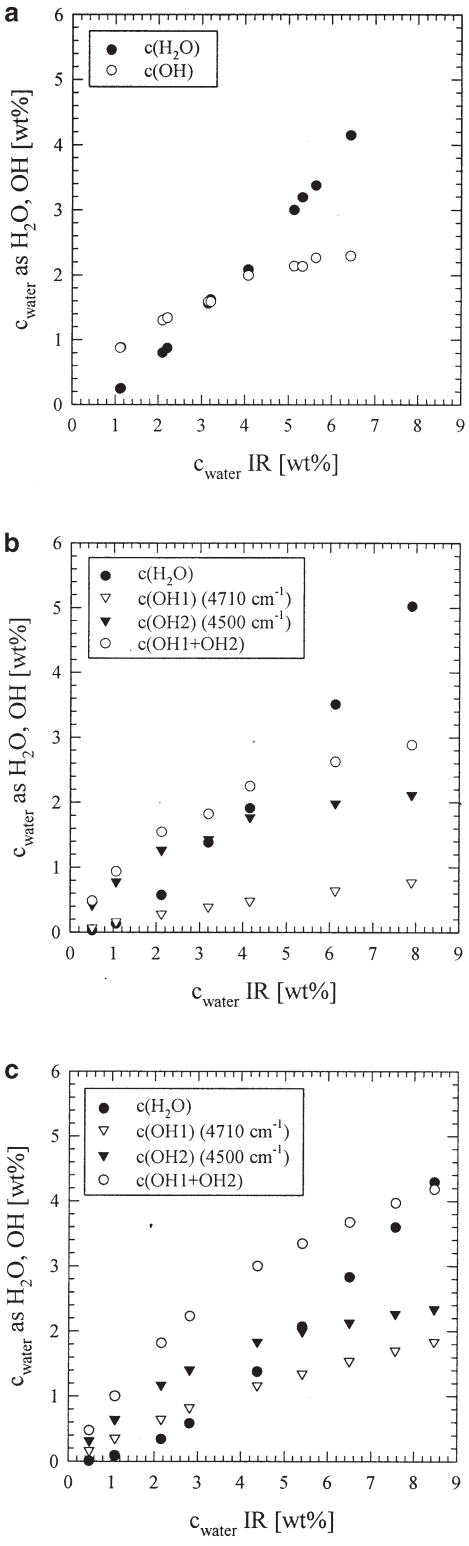

Fig. 9. Water speciation in (a) Ab100-xH, (b) Rd25-xH and (c) Rd100-xH glasses, determined from NIR spectra using the evaluation methods described in the text.

a hydrothermal diamond anvil cell (HDAC) and in-situ NIR spectroscopy. Two HDAC experiments on hydrous Rd100 melts were performed, yielding similar spectroscopic results. However in one of these experiments only the heating cycle up to 800°C could be performed, due to the failure of one of the Mo-heaters at that temperature. Upon heating, spectra were collected every 100 to 200°C, during cooling every 50°C from 800 to 330°C. Below 450°C the sample became less transparent due to the nucleation of bubbles and H_2O exsolution from the melt. Therefore, the liquid-vapour homogenisation temperature could not be determined during cooling. However in the heating-cooling cycle prior to the NIR measurements (with much faster cooling rate), the liquid-vapour homogenisation was observed at about 280°C, resulting in the density of the pressure medium of about 0.75 g/cm^3 (assuming pure H_2O as pressure medium). Thus pressure varied in the temperature interval 800 to 450°C from ~6 to 2 kbar. Another problem that occurred during these experiments was the precipitation of quartz crystals at the gasket rim (determined after the experiments from the recovered gasket with sample) and their growth into the melt, which changed the melt composition to some extent at lower temperatures. Due to the presence of vapour bubbles in the recovered sample, the total water could not be determined from room temperature spectra after the run.

Despite of these experimental problems, some information about the temperature dependence of the water speciation can be extracted from the collected NIR spectra (Fig. 10a). As a control that the total melt water content remained more or less stable during the experiment, the first overtone of the OH stretching vibration at ~7000 cm^{-1} was carefully monitored. Its peak intensity seems to slightly increase with decreasing temperature (especially between 800 and 600°C, Fig. 10b), which is probably related to the increasing density of the melt (note that 800°C is close to the critical temperature for complete miscibility between melt and H_2O for this sample). However, if the melt in the analysed spot would have undergone significant water loss during cooling and corresponding pressure drop (6 to 2 kbar from 800 to 450°C), one would expect a decrease of the 7000 cm^{-1} peak intensity. With increasing temperature the peak intensity of the H_2Omol band at 5230 cm^{-1} decreases significantly, while the intensity of the 4500 cm^{-1} peak seems to increase (Fig. 10a) indicating a conversion of H_2Omol to OH. The peak at 4710 cm^{-1} is less well resolved compared to the 1 atm, room temperature glass spectra. Only at 330°C it is clearly visible but at higher T it develops to a shoulder of the 4500 cm^{-1} peak, which above 600°C cannot clearly be resolved anymore. This behaviour suggests that the 4710 cm^{-1} peak does not significantly increase with increasing T and that the hydroxyl groups represented by this peak (B-OH) are less involved in the H_2Omol conversion reaction. An alternative possibility is that B-OH is indeed involved in this reaction, but the absorption coefficient for the 4710 cm^{-1} has a strong, negative temperature dependence. However, previous in-situ NIR spectroscopic studies suggested no or relatively weak temperature dependencies of the absorption coefficients of water related NIR combination bands for silicate melts (Shen and Keppler, 1995; Nowak and Behrens, 1995; Sowerby and Keppler, 1999). On the other hand Withers et al. (1999) reported some changes of the molar absorptivities with temperature below the glass transition temperature, with the extent of variation being dependent on the choice of the baseline. Nowak and Behrens (2001) reported a strong decrease of ε_{5200} from room temperature glass to high

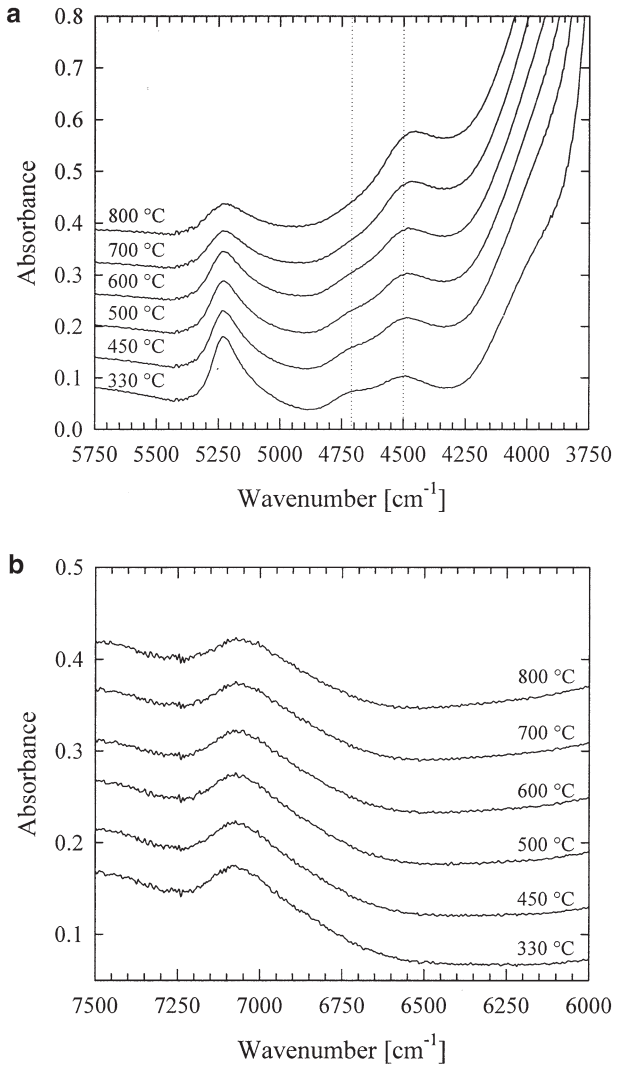

Fig. 10. NIR spectra of hydrous $NaBSi_3O_8$ melt in a hydrothermal diamond anvil cell, (a) NIR combination bands due to H_2Omol and structurally bonded OH; (b) first overtone of the O-H vibration, proportional to total water. The pressure medium had a density of 0.75 g/cm^3, yielding pressures of 6 kbar at 800°C and 2 kbar at 450°C. Spectra were collected during the cooling cycle.

temperature melt, while ε_{4500} increases only slightly. However for a temperature interval of 250°C in the melt, both absorption coefficients seem to be constant. Therefore the explanation that temperature dependencies of the absorption coefficients could explain the observed changes in the high temperature spectra seems to be less likely.

A fully quantitative evaluation of the in-situ NIR spectra measured here was hampered by the background, which underneath the OH combination bands seems to increase due to some broadening of the 4000 cm^{-1} peak. The only reasonable baseline is probably a flexicurve, which however would only be constrained by the high frequency tail of the 4000 cm^{-1} peak and by the flat intensity above 5500 cm^{-1}. In the crucial frequency range of the OH combination bands no constraints are available, thus their intensity determinations would completely depend on the subjective construction of the baseline. For this reason the quantitative determination of the water speciation from the in-situ NIR spectra was not attempted.

Nonetheless, the in-situ spectroscopic investigations revealed important qualitative or semi-quantitative information about the temperature dependence of the water speciation in the melt phase. In accord with previous studies on aluminosilicate melts (Nowak and Behrens, 1995; Shen and Keppler, 1995; Sowerby and Keppler, 1999; Nowak and Behrens, 2001), the fraction of molecular water strongly decreases with increasing temperature and the fraction of hydroxyl groups increases correspondingly, i.e. the equilibrium $H_2O_{melt} + O_{melt} = 2OH_{melt}$ shifts to the right. For example, in the experiment represented in Figure 10, the intensity of the 5200 cm^{-1} peak and thus the amount of H_2Omol reduces by a factor of 0.5 from 450 to 800°C, assuming a temperature independent absorption coefficient for this peak. Only the X-OH peak (4500 cm^{-1}) gains in intensity with increasing *T,* while that of B-OH (4710 cm^{-1}) seems not to change, suggesting that the latter species is less involved in the H_2Omol conversion reaction. This hypothesis is also supported by the annealing experiments presented in the next section.

3.4. Annealing Experiments

As alternative method to in-situ determinations of the water speciation in hydrous melts, annealing experiments at 1 atm were performed with a Rd100 glass containing 2.8 wt.% water (Rd100-2.5H). In these experiments T_f of the glasses can be adjusted to the annealing temperature, i.e. one obtains glasses whose structure and water speciation was frozen at different temperatures (see Dingwell and Webb, 1990, for details). A disadvantage of this method is that only a limited temperature range is available where structural relaxation occurs in a reasonable time frame. An important methodological advantage for the investigated borosilicate melt/glass was that the spectroscopic investigations were performed at room temperature, allowing the same evaluation methods as for the other glasses. Therefore the results are not affected by changing spectral backgrounds or eventual temperature dependencies of the absorption coefficients of the relevant NIR bands. Annealing experiments were performed between 300 and 555°C (Table 3). Below 330°C no equilibrium was reached and at 500°C and higher, the samples lost some water or even foamed. Selected NIR spectra of annealed glasses are given in Figure 11. It is worth noting that the success of the annealing method requires the attainment of equilibrium for the species interconversion. Attainment of equilibrium can unambiguously demonstrated only by reversal experiments, i.e. approaching equilibrium from opposite sides by using samples with different initial species concentrations. This has been done for the glasses annealed at 385/400°C and 435/445°C. Prior to annealing at 385 and 445°C these samples were annealed at 345 and 350°C, so they approached equilibrium from a lower temperature speciation. The 400 and 435°C samples were not annealed before, so they approached equilibrium from a higher temperature speciation. The good agreement of the 385/400°C and 435/445°C data suggests that equilibrium was indeed reached in these experiments (Table 3). For the other glasses more or less constant species concentrations were reached in the time-series experiment, which is indicative for at least near-equilibrium

Table 3. Conditions of annealing experiments (equilibrium data only) and results of NIR spectroscopy.

Annealing T (°C)	Duration[a] (min)	A (5230) (mm^{-1})	A (4710) (mm^{-1})	A (4500) (mm^{-1})	c_{H_2Omol} (wt.%)	c_{OH1} (4710) (wt.%)	c_{OH2} (4500) (wt.%)	c_{water} (wt.%)
333	5040	0.1480	0.1454	0.2136	0.83	0.85	1.25	2.93
345	1110	0.1408	0.1402	0.2142	0.79	0.82	1.25	2.86
350	180–1140	0.1397	0.1454	0.2196	0.78	0.85	1.29	2.92
358	870	0.1398	0.1464	0.2222	0.78	0.86	1.30	2.94
368	300	0.1357	0.1473	0.2307	0.76	0.86	1.35	2.97
385[b]	25–125	0.1265	0.1403	0.2261	0.71	0.82	1.32	2.85
400	10–100	0.1274	0.1442	0.2323	0.71	0.84	1.36	2.92
415	9–60	0.1160	0.1444	0.2415	0.65	0.85	1.41	2.91
430	11	0.1108	0.1410	0.2408	0.62	0.83	1.41	2.86
435	10–40	0.1129	0.1420	0.2420	0.63	0.83	1.42	2.88
445[b]	8–100	0.1080	0.1464	0.2506	0.60	0.86	1.47	2.93
470	4	0.1001	0.1464	0.2546	0.56	0.86	1.49	2.91
487	4	0.0968	0.1378	0.2518	0.54	0.81	1.47	2.82
Unannealed		0.1084	0.1464	0.2496	0.58	0.82	1.41	2.81

[a] Experimental duration after which equilibrium was observed. Note that this duration does not necessarily correspond to the minimum duration for the attainment of equilibrium.

[b] Prior to annealing at 385 and 445°C, these samples were annealed at 345 and 350°C, thus approached equilibrium from a lower temperature speciation.

conditions. The time-series experiments were performed to ensure attainment of equilibrium, but not to study the kinetics of the water species inter-conversion. For this purpose, the time intervals at which NIR spectra were taken should have been much shorter at the beginning of the experiments, where most of the changes took place, to better constrain the time-dependent evolution of the species concentrations.

Figure 12 shows the water speciation in Rd100-2.5H as a function of the annealing temperature. It appears that with increasing temperature the concentration of H_2Omol decreases, while that of X-OH (represented by the peak at 4500 cm^{-1}) increases correspondingly. The B-OH concentration remains constant within experimental and analytical error. These data confirm the conclusions drawn from the in-situ experiments, namely that the fraction of hydroxyl groups increases on cost of molecular water with increasing temperature. Considering equilibrium between H_2Omol, X-OH and B-OH, the data further suggest that B-OH participate to a much smaller extent in the H_2Omol conversion reaction than X-OH. Assuming ideal mixing of the different water species with the silicate network the equilibrium constant (k) of the reaction $H_2O_{melt} + O_{melt} = 2OH_{melt}$ is given by

$$k = \frac{[OH]^2}{[O] \cdot [H_2O]}, \quad (3)$$

where [OH], [O] and [H_2O] are the mole fractions of OH, anhydrous O and H_2O on a single oxygen basis (e.g. Stolper,

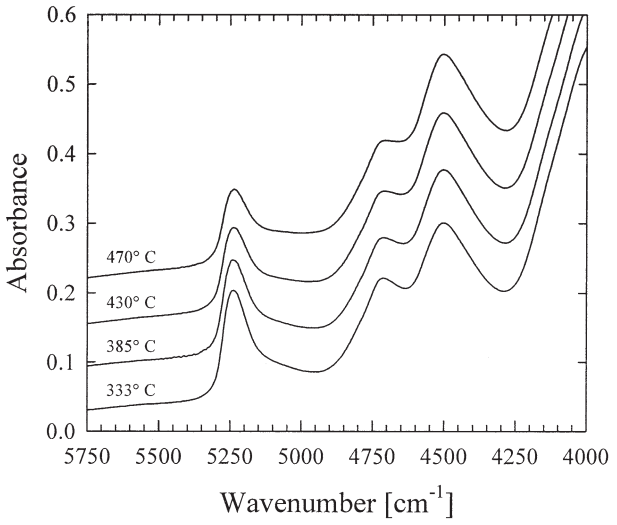

Fig. 11. NIR spectra of Rd100-2.5H glasses (~2.8 wt.% water) annealed at various temperatures.

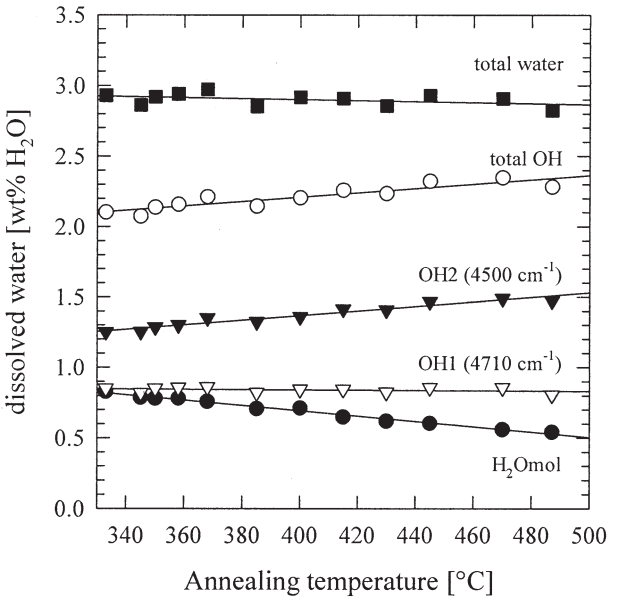

Fig. 12. Evolution of the water speciation in Rd100 glasses containing 2.8 wt.% water as a function of the annealing temperature (corresponding to the fictive temperature of the samples).

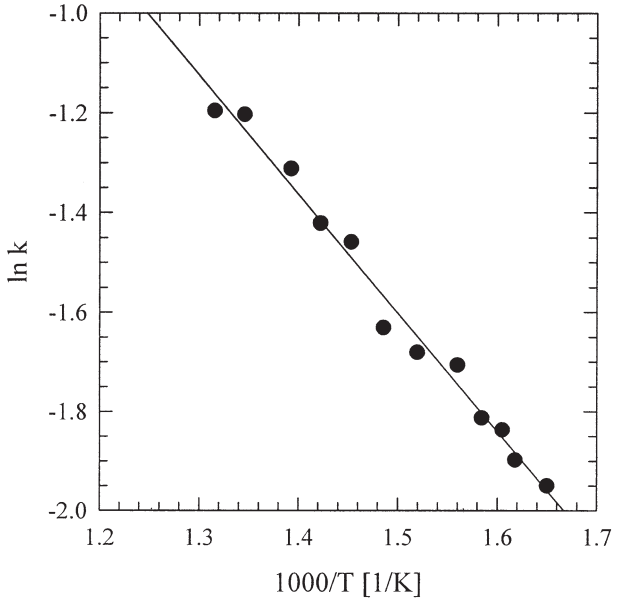

Fig. 13. Temperature dependence of the equilibrium constant k and fitting the experimental data to the function $\ln k = a + b/T$. The fit parameters $a = 1.98$ and $b = -2388$ yield an enthalpy and entropy of the reaction $H_2O_{melt} + O_{melt} = 2OH_{melt}$ of $\Delta H° = 19.9$ kJ/mol and $\Delta S° = 16.5$ J/mol · K.

1982). As the conversion reaction affects mainly X-OH groups represented by the 4500 cm^{-1} peak, the concentrations of B-OH groups (4710 cm^{-1}) were not considered in the calculation (thus, [OH] refers to X-OH). By plotting ln(k) versus reciprocal temperature (Fig. 13) the enthalpy ($\Delta H°$) and entropy ($\Delta S°$) of the conversion reaction were determined to be 19.9 kJ/mol and $\Delta S° = 16.5$ J/mol · K, respectively. These numbers are considerably lower than those determined previously with in-situ NIR spectroscopy for aluminosilicate melts ($\Delta H° = 27$–36 kJ/mol, $\Delta S° = 18$–30 J/mol · K, e.g. Nowak and Behrens, 1995; Shen and Keppler, 1995; Sowerby and Keppler, 1999, 2000; Nowak and Behrens, 2001) and with controlled cooling experiments (Romano et al. 1995b). Water speciation data obtained from annealing experiments gave lower $\Delta H°$ and $\Delta S°$ (e.g. $\Delta H° = 25.9 \pm 0.4$ kJ/mol, $\Delta S° = 15.7 \pm 0.4$ J/mol · K, Zhang et al., 1997; Ihinger et al., 1999). The reasons for these discrepancies are not fully clear yet and were discussed in greater detail in Nowak and Behrens (2001) and Behrens and Nowak (2003). The reason for the particularly low $\Delta H°$ and $\Delta S°$ values presented here may partly lie in the applied NIR evaluation method, which probably overestimates the OH concentrations (particularly those of X-OH). If the measured intensities at 4500 cm^{-1} contain contributions from other bands (e.g. high frequency tails of the 4000–4100 and 3600 cm^{-1} peaks), the relative change of the X-OH peak with temperature and thus the extent of the H_2O conversion reaction will be underestimated, thus leading to reduced $\Delta H°$ and $\Delta S°$ values. However, the different chemical composition compared to previous studies (borosilicate vs. aluminosilicate) may not only affect the room temperature water speciation, but also its temperature dependence.

4. CONCLUSIONS

NIR spectroscopy indicates the presence of additional water species in boro(alumino)silicate glasses (compared to aluminosilicate glasses) through the appearance of combination bands at 4640 and 4710 cm^{-1}. It is suggested that these peaks are due to B-OH complexes. From ^{II}B MAS NMR spectroscopy it is known that ^{II}B is the dominating species in hydrous $NaAlSi_3O_8 + B_2O_3$ glasses (Schmidt et al., 2004) and B^{IV} is the dominating species in hydrous $NaAlSi_3O_8$-$NaBSi_3O_8$ glasses (Schmidt and Dupree, 2002). The frequency difference of the "B-OH peak" in the NIR spectra (4640 vs. 4710 cm^{-1}) may reflect hydroxyls attached to BO_3 and BO_4 polyhedra. Other (spectroscopic) methods are desired to verify these tentative assignments. NIR spectroscopy demonstrates furthermore that in (alumino)silicate glasses boron significantly stabilises hydroxyl groups at the expense of molecular H_2O. The formation of additional B-OH complexes tentatively explains the increased water solubility in B-bearing melts and glasses (Pichavant 1981; Holtz et al., 1993; Romano et al., 1995a). However, the additional complexity in the NIR spectra renders reliable spectra evaluation much more difficult. Therefore, extracted water species concentrations have significantly higher uncertainties compared to B-free glasses. Aside of testing different approaches for the baseline construction, it is important to better constrain the NIR absorption coefficients of the different OH-related peaks, i.e. an independent determination of ε(B-OH) and ε(X-OH) is necessary. This could be facilitated by other spectroscopic methods that are capable of determining at least relative H_2Omol and total OH concentrations. If such data were available, independent extinction coefficients for B-OH and X-OH could be determined.

Both, in-situ NIR spectroscopy on hydrous Rd100 melt and annealing experiments show that the water speciation changes towards OH groups with increasing temperature (at the expense of molecular H_2O). The $H_2O \rightarrow$ OH conversion produces dominantly OH groups, which are represented by the 4500 cm^{-1} NIR band. The concentration of B-OH complexes (represented by the 4710 cm^{-1} NIR peak) seems to be much less temperature dependent.

Acknowledgements—The author appreciated the careful sample preparations of Oskar Leitner and Hubert Schulze and interesting discussions with Fabrice Gaillard. The author thanks Prof. Ray Dupree for access to the NMR facilities at Warwick University, UK, for quantitative determination of water contents. This research was carried out with the financial support of the Bayerisches Geoinstitut and the DFG Schwerpunktprogramm "Bildung, Transport und Differenzierung von Silikatschmelzen", SPP 1055, Schm 1622/1. The manuscript benefited from the comments and suggestions of Claudia Romano, Anthony Withers and an anonymous reviewer.

Associate editor: C. Romano

REFERENCES

Acocella J., Tomozawa M., and Watson E. B. (1984) The nature of dissolved water in silicate glasses and its effect on various properties. *J. Non-Cryst. Solids* **65,** 355–372.

Bartholomew R. F. and Schreurs J. W. H. (1980) Wide-line NMR study of protons in hydrosilicate glasses of different water content. *J. Non-Cryst. Solids* **38 & 39,** 679–684.

Basset W. A., Shen A. H., Bucknum M., and Chou I.-M. (1993) A new diamond anvil cell for hydrothermal studies to 2.5 GPa and from 190 to 1200° C. *Rev. Sci. Instrum.* **64,** 2340–2345.

Behrens H. and Nowak M. (2003) Quantification of H_2O speciation in silicate glasses and melts by IR spectroscopy — In-situ versus quench techniques. *Phase Transitions* **76,** 45–61.

Behrens H., Romano C., Nowak M., Holtz F., and Dingwell D. B. (1996) Near-infrared spectroscopic determination of water species in glasses of the system $MAlSi_3O_8$ (M = Li, Na, K): An interlaboratory study. *Chem. Geol.* **128,** 41–63.

Chorlton L. B. and Martin R. F. (1978) The effect of boron on the granite solidus. *Can. Mineral.* **16,** 239–244.

Dingwell D. B. and Webb S. L. (1990) Relaxation in silicate melts. *Eur. J. Mineral.* **2,** 427–449.

Dingwell D. B., Knoche R., Webb S. L., and Pichavant M. (1992) The effect of B_2O_3 on the viscosity of haplogranitic melts. *Am. Mineral.* **77,** 457–461.

Dingwell D. B., Pichavant M., and Holtz F. (1996) Experimental studies of boron in granitic melts. In *Boron, Mineralogy, Petrology and Geochemistry* (*Reviews in Mineralogy 33;* eds. E. Grew and L. Arovitz). Mineral. Soc. Am., Washington, DC, pp. 331–385.

Eckert H., Yesinowski J. P., Silver L. A., and Stolper E. M. (1988) Water in silicate glasses: Quantification and structural studies by ^1H solid echo and MAS-NMR techniques. *J. Phys. Chem.* **92,** 2055–2064.

Holtz F., Behrens H., and Dingwell D. B. (1993) The effects of fluorine, boron and phosphorus on the solubility of water in haplogranitic melts compared to natural silicate melts. *Contrib. Mineral. Petrol.* **113,** 492–501.

Ihinger P. D., Zhang Y., and Stolper E. M. (1999) The speciation of dissolved water in rhyolitic melt. *Geochim. Cosmochim. Acta* **63,** 3567–3578.

London D. (1997) Estimating abundances of volatile and other mobile components in evolved silicic melts through mineral-melt equilibria. *J. Petrol.* **38,** 1691–1706.

Newman S., Stolper E. M., and Epstein S. (1986) Measurement of water in rhyolitic glasses: Calibration of an infrared spectroscopic technique. *Am. Mineral.* **71,** 1527–1541.

Nowak M. and Behrens H. (1995) The speciation of water in haplogranitic glasses and melts determined by in situ near-infrared spectroscopy. *Geochim. Cosmochim. Acta* **59,** 3445–3450.

Nowak M. and Behrens H. (1997) An experimental investigation on diffusion of water in haplogranitic melts. *Contrib. Mineral. Petrol.* **126,** 365–376.

Nowak M. and Behrens H. (2001) Water in rhyolitic magmas: Getting a grip on a slippery problem. *Earth Planet. Sci. Lett.* **184,** 515–522.

Ohlhorst S., Behrens H., and Holtz F. (2001) Compositional dependence of molar absorptivities of near-infrared OH- and H_2O bands in rhyolitic to basaltic glasses. *Chem. Geol.* **174,** 5–20.

Pichavant M. (1981) An experimental study of the effect of boron on a water-saturated haplogranite at 1 kbar pressure: Geological applications. *Contrib. Mineral. Petrol.* **76,** 430–439.

Pichavant M. (1987) Effects of B and H_2O on liquidus phase relations in the haplogranite system at 1 kbar. *Am. Mineral.* **72,** 1056–1070.

Romano C., Dingwell D. B., and Hess K. U. (1995a) The effect of boron on the speciation of water in haplogranitic melts. *Per. Mineral.* **64,** 413–431.

Romano C., Dingwell D. B., and Behrens H. (1995b) The temperature dependence of the speciation of water in $NaAlSi_3O_8$ - $KAlSi_3O_8$ melts: An application of fictive temperatures derived from synthetic fluid-inclusions. *Contrib. Mineral. Petrol.* **122,** 1–10.

Schmidt B. C., Behrens H., Riemer T., Kappes R., and Dupree R. (2001) Quantitative determination of water speciation in aluminosilicate glasses: A comparative NMR and IR spectroscopic study. *Chem. Geol.* **174,** 195–208.

Schmidt B. C. and Dupree R. (2002) Effect of water on the structure of melts and glasses along the join $NaAlSi_3O_8$-$NaBSi_3O_8$. EOS Trans. AGU, 83(47) Fall Meet. Suppl., Abstract V72B-1318.

Schmidt B. C., Zotov N., and Dupree R. (2004) Structural implications of water and boron dissolution in albite glass. *J. Non-Cryst. Solids.* **337,** 207-219.

Scholze H. (1960) Zur Frage der Unterscheidung zwischen H_2O Molekeln und OH-Gruppen in Gläsern und Mineralen. *Naturwissenschaften* **47,** 226–227.

Shen A. and Keppler H. (1995) Infrared spectroscopy of hydrous silicate melts to 1000° C and 10 kbar: Direct observation of H_2O speciation in a diamond-anvil cell. *Am. Mineral.* **80,** 1335–1338.

Silver L. and Stolper E. (1989) Water in albitic glasses. *J. Petrol.* **30,** 667–709.

Silver L. A., Ihinger P. D., and Stolper E. (1990) The influence of bulk composition on the speciation of water in silicate glasses. *Contrib. Mineral. Petrol.* **104,** 142–162.

Sowerby J. R. and Keppler H. (1999) Water speciation in rhyolitic melt determined by in-situ infrared spectroscopy. *Am. Mineral.* **84,** 1843–1849.

Sowerby J. R., and Keppler H. (2000) Erratum to "Water speciation in rhyolitic melt determined by in-situ infrared spectroscopy". *Am. Mineral.* **85,** 880.

Stolper E. (1982) Water in silicate glasses: An infrared spectroscopic study. *Contrib. Mineral. Petrol.* **81,** 1–17.

Stolper E. (1989) Temperature dependence of the speciation of water in rhyolitic melts and glasses. *Am. Mineral.* **74,** 1247–1257.

Thomas R., Förster H.-J., and Heinrich W. (2003) The behaviour of boron in a peraluminous granite-pegmatite system and associated hydrothermal solutions: A melt and fluid-inclusion study. *Contrib. Mineral. Petrol.* **144,** 457–472.

Withers A. C. and Behrens H. (1999) Temperature induced changes in the NIR spectra of hydrous albitic and rhyolitic glasses between 300 and 100 K. *Phys. Chem. Mineral.* **27,** 119–132.

Withers A. C., Zhang Y., and Behrens H. (1999) Reconciliation of experimental results on H_2O speciation in rhyolitic glass using in-situ and quenching techniques. *Earth Planet. Sci. Lett.* **173,** 343–349.

Wu C. K. (1980) Nature of incorporated water in hydrated silicate glasses. *J. Am. Ceram. Soc.* **63,** 453–457.

Zhang Y., Xu Z., and Behrens H. (2000) Hydrous species geospeedometer in rhyolite: Improved calibration and application. *Geochim. Cosmochim. Acta* **64,** 3347–3355.

Zhang Y., Stolper E. M., and Ihinger P. D. (1995) Kinetics of the reaction $H_2O + O = 2OH$ in rhyolitic and albitic glasses: Preliminary results. *Am. Mineral.* **80,** 593–612.

Zhang Y., Belcher R., Ihinger P. D., Wang L., Xu Z., and Newman S. (1997) New calibration of infrared measurements of dissolved water in rhyolitic glasses *Geochim. Cosmochim. Acta* **61,** 3089–3100.